Mga2 transcription factor regulates an oxygen-responsive lipid homeostasis pathway in fission yeast

Burr, Risa; Stewart, Emerson V; Shao, Wei; Zhao, Shan; Hannibal-Bach, Hans Kristian; Ejsing, Christer S.; Espenshade, Peter J

Published in:
Journal of Biological Chemistry

DOI:
10.1074/jbc.M116.723650

Publication date:
2016

Document version
Publisher's PDF, also known as Version of record

Citation for pulished version (APA):
Burr, R., Stewart, E. V., Shao, W., Zhao, S., Hannibal-Bach, H. K., Ejsing, C. S., & Espenshade, P. J. (2016). Mga2 transcription factor regulates an oxygen-responsive lipid homeostasis pathway in fission yeast. Journal of Biological Chemistry, 291(23), 12171-12183. DOI: 10.1074/jbc.M116.723650

THE JOURNAL OF BIOLOGICAL CHEMISTRY VOL. 291, NO. 23, pp. 12171–12183, June 3, 2016

Mga2 Transcription Factor Regulates an Oxygen-responsive Lipid Homeostasis Pathway in Fission Yeast*[S]

Received for publication, February 24, 2016, and in revised form, April 1, 2016 Published, JBC Papers in Press, April 6, 2016, DOI 10.1074/jbc.M116.723650

Risa Burr[‡], Emerson V. Stewart[‡], Wei Shao[‡], Shan Zhao[‡], Hans Kristian Hannibal-Bach[§], Christer S. Ejsing[§], and Peter J. Espenshade[‡1]

From the [‡]Department of Cell Biology, The Johns Hopkins University School of Medicine, Baltimore, Maryland 21205 and the [§]Department of Biochemistry and Molecular Biology, VILLUM Center for Bioanalytical Sciences, University of Southern Denmark, 5230 Odense, Denmark

Eukaryotic lipid synthesis is oxygen-dependent with cholesterol synthesis requiring 11 oxygen molecules and fatty acid desaturation requiring 1 oxygen molecule per double bond. Accordingly, organisms evaluate oxygen availability to control lipid homeostasis. The sterol regulatory element-binding protein (SREBP) transcription factors regulate lipid homeostasis. In mammals, SREBP-2 controls cholesterol biosynthesis, whereas SREBP-1 controls triacylglycerol and glycerophospholipid biosynthesis. In the fission yeast *Schizosaccharomyces pombe*, the SREBP-2 homolog Sre1 regulates sterol homeostasis in response to changing sterol and oxygen levels. However, notably missing is an SREBP-1 analog that regulates triacylglycerol and glycerophospholipid homeostasis in response to low oxygen. Consistent with this, studies have shown that the Sre1 transcription factor regulates only a fraction of all genes up-regulated under low oxygen. To identify new regulators of low oxygen adaptation, we screened the *S. pombe* nonessential haploid deletion collection and identified 27 gene deletions sensitive to both low oxygen and cobalt chloride, a hypoxia mimetic. One of these genes, *mga2*, is a putative transcriptional activator. In the absence of *mga2*, fission yeast exhibited growth defects under both normoxia and low oxygen conditions. Mga2 transcriptional targets were enriched for lipid metabolism genes, and *mga2*Δ cells showed disrupted triacylglycerol and glycerophospholipid homeostasis, most notably with an increase in fatty acid saturation. Indeed, addition of exogenous oleic acid to *mga2*Δ cells rescued the observed growth defects. Together, these results establish Mga2 as a transcriptional regulator of triacylglycerol and glycerophospholipid homeostasis in *S. pombe*, analogous to mammalian SREBP-1.

Oxygen is required for sterol synthesis and fatty acid desaturation (1–3). Therefore, cells need to adapt lipid supply to oxygen availability. Mammalian cells respond to changing lipid availability through a conserved family of ER[2] membrane-bound SREBP transcription factors. SREBPs are bound and regulated by Scap, a multiple pass transmembrane protein that senses sterols (4, 5). Under conditions of low sterols, Scap transports SREBPs from the ER to the Golgi, where they are consecutively cleaved by the site-1 and site-2 proteases, producing an active N-terminal transcription factor fragment (SREBP-N) (6). This cleavage releases the SREBP-N transcription factor domain to enter the nucleus and up-regulate transcription of target genes. In mammals, there are three isoforms of SREBP. SREBP-1 (a and c) regulate TAG and glycerophospholipid synthesis through target genes, including fatty-acid synthase, stearoyl-CoA desaturase, and long chain fatty acid-CoA ligase (4). SREBP-2 regulates cholesterol biosynthesis through genes such as HMG-CoA synthase, HMG-CoA reductase, and CYP51, as well as cholesterol uptake through control of LDL receptor expression (4, 7).

We showed previously that fission yeast contains functional SREBP transcription factors, most notably Sre1 (8, 9). Sre1 regulates ergosterol homeostasis in a way that is analogous to SREBP-2; activation of Sre1 requires transport from the ER to the Golgi, where the N-terminal transcription factor domain is released from the anchoring transmembrane domains (8, 9). Interestingly, Sre1 also regulates a low oxygen response, representing the sole low oxygen-responsive program described in *Schizosaccharomyces pombe* (8, 9). Under low oxygen, ergosterol synthesis becomes limiting. Sre1 up-regulates transcription of the oxygen-dependent enzymes in ergosterol synthesis and as a consequence restores ergosterol levels, allowing the cell to adapt to a low oxygen environment (8).

Characterization of the low oxygen-responsive pathways in fission yeast has implications for treatment of fungal infections. Sites of fungal infection are hypoxic, and fungal pathogens require SREBP to adapt to these conditions and remain virulent, demonstrating conservation of this low oxygen-responsive pathway across yeast species (10). Consequently, the SREBP pathway is an important antifungal drug target (10–13). Notably, Sre1 regulates only a fraction of oxygen-responsive genes in fission yeast. Our previous study identified 404 genes that are

* This work was supported by National Institutes of Health Grant HL077588 (to P. J. E.) and VILLUM FONDEN Grant VKR023439 (to C. S. E.). The authors declare that they have no conflicts of interest with the contents of this article. The content is solely the responsibility of the authors and does not necessarily represent the official views of the National Institutes of Health.
[S] This article contains supplemental Tables S1–S6.
[1] To whom correspondence should be addressed: Dept. of Cell Biology, The Johns Hopkins University School of Medicine, 725 N. Wolfe St., Physiology 107B, Baltimore, MD 21205. Tel.: 443-287-5026; Fax: 410-502-7826; E-mail: peter.espenshade@jhmi.edu.

[2] The abbreviations used are: ER, endoplasmic reticulum; SREBP, sterol regulatory element-binding protein; Scap, SREBP cleavage-activating protein; YES, yeast extract plus supplements; $CoCl_2$, cobalt chloride; SAM, significance analysis of microarrays; TAG, triacylglycerol; PA, phosphatidic acid; PE, phosphatidylethanolamine; MIPC, mannosylinositol phosphorylceramide; qPCR, quantitative PCR.

TABLE 1
***S. pombe* strain list**

Strains	Genotype	Source	Figs.
ED666	*h+ leu1-32 ura4-D18 ade6-M210*	Bioneer Inc.	1
Deletion strains	*h+ leu1-32 ura4-D18 ade6-M210* Δ[*GOI*]-*D1*::*kanMX4*	Bioneer Inc.	1
KGY425	*h− leu1-32 ura4-D18 ade6-M210 his3-D1*	ATCC	1–5
PEY522	*h− leu1-32 ura4-D18 ade6-M210 his3-D1* Δ*sre1-D1*::*kanMX6*	8	1
PEY1762	*h− leu1-32 ura4-D18 ade6-M210 his3-D1* Δ*mga2-D1*::*kanMX6*	This study	1–5
PEY875	*h− leu1-32 ura4-D18 ade6-M210 his3-D1 sre1N*	28	1 and 2
PEY1763	*h+ leu1-32 ura4-D18 ade6-M210 his3-D1* Δ*mga2-D1*::*kanMX6*	This study	1 and 2
PEY1764	*h+ leu1-32 ura4-D18 ade6-M210 his3-D1* Δ*mga2-D1*::*kanMX6 sre1N*	This study	1 and 2

up-regulated under low oxygen but are not Sre1 targets (9). Therefore, additional low oxygen-responsive pathways remain to be discovered. Given that fission yeast adaptation to low oxygen is a model for low oxygen responses in pathogenic fungi, identification of these pathways could highlight novel targets for inhibitors of fungal pathogenesis (14–17).

Here, we report the results of a screen of 2601 fission yeast non-essential haploid deletion mutants for genes required for growth in low oxygen and in the presence of cobalt chloride. In this report, we define Mga2 as a transcriptional activator required for growth under both low oxygen and cobalt chloride conditions. *mga2* has homologs in *Saccharomyces cerevisiae* that are ER membrane-bound transcriptional activators required for expression of the Δ9 fatty acid desaturase *OLE1* (18, 19). We demonstrate that fission yeast Mga2 regulates a low oxygen-responsive gene expression program distinct from Sre1. Genes regulated by Mga2 include the fatty-acid synthases *fas1* and *fas2*, the fatty acid desaturase *ole1*, and the long chain fatty acid CoA ligase *lcf1*, all of which are homologs of SREBP-1 targets in mammals. We find that *mga2* is required to maintain TAG and glycerophospholipid homeostasis. Therefore, Mga2 regulates a second low oxygen response pathway in *S. pombe* that is analogous to the function of SREBP-1 in mammals.

Experimental Procedures

Materials—We obtained general chemicals and materials from Sigma or Fisher. Other sources include the following: yeast extract, peptone, and agar from BD Biosciences; *S. pombe* haploid deletion collection version 1 from Bioneer; cobalt(II) chloride and amino acid supplements from Roche Applied Science; Moloney murine leukemia virus reverse transcriptase from New England Biolabs; RNA STAT-60 from Tel-Test; GoTaq qPCR Master Mix from Promega; oligonucleotides from Integrated DNA Technologies; horseradish peroxidase-conjugated, affinity-purified donkey anti-rabbit IgG from Jackson ImmunoResearch; IRDye donkey anti-rabbit and from Li-Cor; prestained protein standards from Bio-Rad; and fatty acid-free bovine serum albumin from SeraCare Life Sciences.

Antibodies—Rabbit polyclonal antibody against amino acids 1–260 of Sre1 (anti-Sre1 IgG) was generated using a standard protocol as described previously; we purified the antigen with an N-terminal polyhistidine tag and a tobacco etch virus protease cleavage sequence from *Escherichia coli* using nickel-nitrilotriacetic acid-agarose (Qiagen). We then cleaved with tobacco etch virus protease (Invitrogen) to remove the histidine tag. We isolated Sre1-specific antibodies from rabbit serum by affinity chromatography using NHS-Sepharose resin (Pierce) conjugated to the polyhistidine-tagged Sre1 antigen (8). Specificity of this antibody was assayed by loss of immunoreactivity in an *sre1*Δ strain.

We generated monoclonal antibody 5B4 IgG1κ to Sre1 (amino acids 1–260) using recombinant protein that was purified from *E. coli* by nickel-affinity chromatography (Qiagen). We immunized BALB/c mice with this antigen and screened for immunoreactivity by ELISA and Western blotting. We fused spleen cells from immunopositive mice with SP2/0 myeloma cells to make monoclonal antibodies. We identified positive clones by ELISA screening using the immunizing antigen. After dilution cloning, antibody specificity was tested by immunoblotting against *S. pombe* extracts from cells overexpressing Sre1. We determined isotype using the mouse isotyping kit (Roche Applied Science). We purified final antibodies from either tissue culture supernatant or ascites fluid using protein-G-Sepharose (GE Healthcare).

Yeast Culture—Yeast strains are described in Table 1. *S. pombe* cells were grown to exponential phase at 30 °C in rich YES medium (0.5% (w/v) yeast extract plus 3% (w/v) glucose supplemented with 225 μg/ml each of uracil, adenine, leucine, histidine, and lysine (20)). YES + $CoCl_2$ medium was prepared by dissolving cobalt(II) chloride in H_2O and adding to a final concentration of 1.6 mM in YES medium. For fatty acid supplementation, fatty acids were added to 1 mM in YES medium from a 12.7 mM stock in 12% (w/v) fatty acid-free BSA.

BSA Conjugation of Free Fatty Acids—Fatty acid-free BSA (24% w/v) was made by adding 12 g of fatty acid-free bovine serum albumin to 35 ml of 150 mM NaCl in six 2-g doses over 5 h. pH was adjusted to 7.4 with 5 N NaOH, and the volume was brought up to 50 ml with 150 mM NaCl. This solution was diluted 1:1 with 150 mM NaCl to produce 12% fatty acid-free BSA prior to use as an experimental control.

Fatty acid conjugation to BSA was performed by dissolving 319 μmol of the conjugating fatty acid in 2 ml of EtOH. 100 μl of 5 N NaOH was added to precipitate sodium salt of the fatty acid. EtOH was evaporated under nitrogen gas. 10 ml of 150 mM NaCl were added to the dried fatty acid, and the solution was heated until the fatty acid dissolved. The solution was then stirred and slowly cooled to just before the fatty acid precipitated, at which point 12.5 ml of ice-cold fatty acid-free BSA (24% w/v) was added. The solution was stirred for 10 min, and the final volume was adjusted to 25 ml with 150 mM NaCl.

S. pombe Deletion Collection Screen—The Bioneer Haploid Deletion Mutant Library version 1.0 was screened as described previously (21). 2601 deletion mutants were streaked for single colonies on YES or YES + $CoCl_2$ medium and placed at 30 °C in the presence of oxygen. An additional YES plate was grown at

30 °C in anaerobic conditions using the BBL GasPak system (BD Biosciences). Mutants were compared with wild-type and *sre1*Δ strains and scored for growth after 7 days. Full screen results can be found in supplemental Table S1.

Sre1 Cleavage Assay—Cells were grown in YES medium to exponential phase inside an InVivo$_2$ 400 hypoxic work station (Biotrace, Inc.) and collected for protein extraction and immunoblotting as described previously using polyclonal or monoclonal 5B4 anti-Sre1 antibody as indicated (8). SDS-polyacrylamide gels were equally loaded for total protein, which was quantified using the BCA protein assay (Pierce). Consistent loading was confirmed following electroblotting by staining the membrane with Ponceau S. Blots were imaged using enhanced chemiluminescence and film or the Odyssey CLx infrared imaging system (Li-Cor), as noted in the figure legends.

Microarray—Data in supplemental Tables S4 and S5 represent the log2 fold changes in expression between *sre1*Δ and *sre1*Δ *mga2*Δ cells grown anaerobically for 1.5 h. Microarray analysis was performed as described previously (11). Total RNA was isolated using RNA STAT-60 and amplified and labeled using the RNA amplification and labeling kit (Agilent Technologies) with oligo(dT) primers (System Bioscience) and cyanine CTPs (PerkinElmer Life Sciences). RNA was fragmented, denatured, and hybridized to a custom Agilent array at 60 °C for 17 h. Two dye-reversal hybridizations were performed with cells cultured on different days (biological replicates), yielding two data points per probe. Arrays were scanned by an Agilent G2505B scanner, and features were flagged using Agilent Feature Extraction software. These data were imported into Partek Genomics Suite as the median of the arrays' three replicate probes' g/r processed signals. These log2 signal values were quantile-normalized, and the dye-swapped samples were compared in a one-way ANOVA. Because there were only two biological replicates, a pseudo *p* value is presented alongside a significance analysis of microarrays (SAM) *q*-value. SAM parameters were Δ = 1.87646, false discovery rate (median) = 0.05447. Mga2-dependent genes showed lower expression in *sre1*Δ *mga2*Δ *versus sre1*Δ cells. The microarray gene expression data described in this study have been deposited in the NCBI Gene Expression Omnibus (22) and are accessible through GEO Series accession number GSE60544.

Quantitative PCR—Yeast cells (1×10^8) growing exponentially in the presence or absence of oxygen were pelleted, resuspended in RNA STAT 60, and vortexed. Samples were mixed with chloroform to 16% (v/v) and then centrifuged at 10,000 × *g* for 15 min at 4 °C. The aqueous fraction was mixed with isopropyl alcohol to 33% (v/v) and then centrifuged at 10,000 × *g* for 10 min. Precipitated RNA was washed with 75% (v/v) EtOH and air-dried. cDNA was synthesized following DNase and reverse transcription instructions for Moloney murine leukemia virus reverse transcriptase. RT-qPCR was performed using the indicated primers and GoTaq qPCR Master Mix. Each reaction was performed with two technical replicates per the five biological replicates. Error bars are 1 S.D.

Lipid Extraction—Lipid extraction was performed as described previously (23–25). Six biological replicate cultures of wild-type and *mga2*Δ cells growing exponentially in the presence of oxygen (6.8×10^7–1.3×10^8 cells) were pelleted and washed twice in 155 mM ammonium acetate and then frozen under liquid nitrogen. Lipids were extracted at 4 °C by breaking cell pellet with beads, and then 20 internal lipid standards were added to the lysate. Samples were subjected to two-step extraction with chloroform/methanol. The collected lipid extracts were then vacuum-evaporated and dissolved in chloroform/methanol.

Shotgun Lipidomics—Mass spectrometry was performed as described previously (23–25). Extracts were analyzed on a LTQ Orbitrap XL mass spectrometer (Thermo Fisher Scientific) equipped with the robotic nanoflow ion source TriVersa NanoMate (Advion Biosciences).

Lipidomics Data Analysis—Lipidomics data analysis was performed as described previously using ALEX software (24, 25). Species were annotated using sum composition as follows: ⟨lipid class⟩⟨total number of carbons in the fatty acid moieties⟩:⟨total number of double bonds in the fatty acid moieties⟩. Sphingolipids were annotated as ⟨lipid class⟩⟨total number of carbons in the long-chain base and fatty acid moiety⟩:⟨total number of double bonds in the long-chain base and fatty acid moiety⟩;⟨total number of OH groups in the long-chain base and fatty acid moiety⟩. Visualization and calculation of mole % values were performed using the commercially available Tableau software. *p* values were calculated using a Mann-Whitney *U* test. *p* values were corrected for multiple hypotheses post hoc using the Benjamini and Hochberg false discovery rate (26). Equations 1–3 were utilized to calculate the presented mole % values, where *n* is molar abundance of lipid species *i* belonging to lipid class *j*,

$$\text{mol \% of lipid species per all lipids} = \frac{n_{ij}}{\Sigma\Sigma(n_{ij})} \times 100 \quad \text{(Eq. 1)}$$

$$\text{mol \% of lipid species per lipid class} = \frac{n_{ij}}{\Sigma(n_{ij})} \times 100 \quad \text{(Eq. 2)}$$

$$\text{mol \% of monounsaturated fatty acids per lipid class} = \frac{\Sigma(n_{ij} \times \#\text{ double bonds})}{\Sigma(n_{ij} \times \#\text{ acyl chains per lipid molecule})} \times 100 \quad \text{(Eq. 3)}$$

Equation 3 was calculated based on the fact that that *S. pombe* only synthesizes saturated and mono-unsaturated fatty acids (27). In the case where fatty acid saturation was determined, lipid species were hydrolyzed *in silico* prior to normalization (25). For example, for TAG 42:2, two of the fatty acid moieties must be monounsaturated and one must be saturated; this is taken into account when tabulating the number of saturated and unsaturated fatty acids across all TAG species. The supplemental Table S6 lists the full results of the lipidomics analysis.

Results

Identification of Genes Required for Growth under Low Oxygen and on Cobalt Chloride—Adaptation to low oxygen in fission yeast requires the coordinated regulation of many genes (9). The Sre1 transcription factor only regulates expression of 22% of low oxygen-responsive genes, suggesting that additional oxygen-regulated transcription factors exist (9). Successful low oxygen adaptation can be assayed by growth of fission yeast

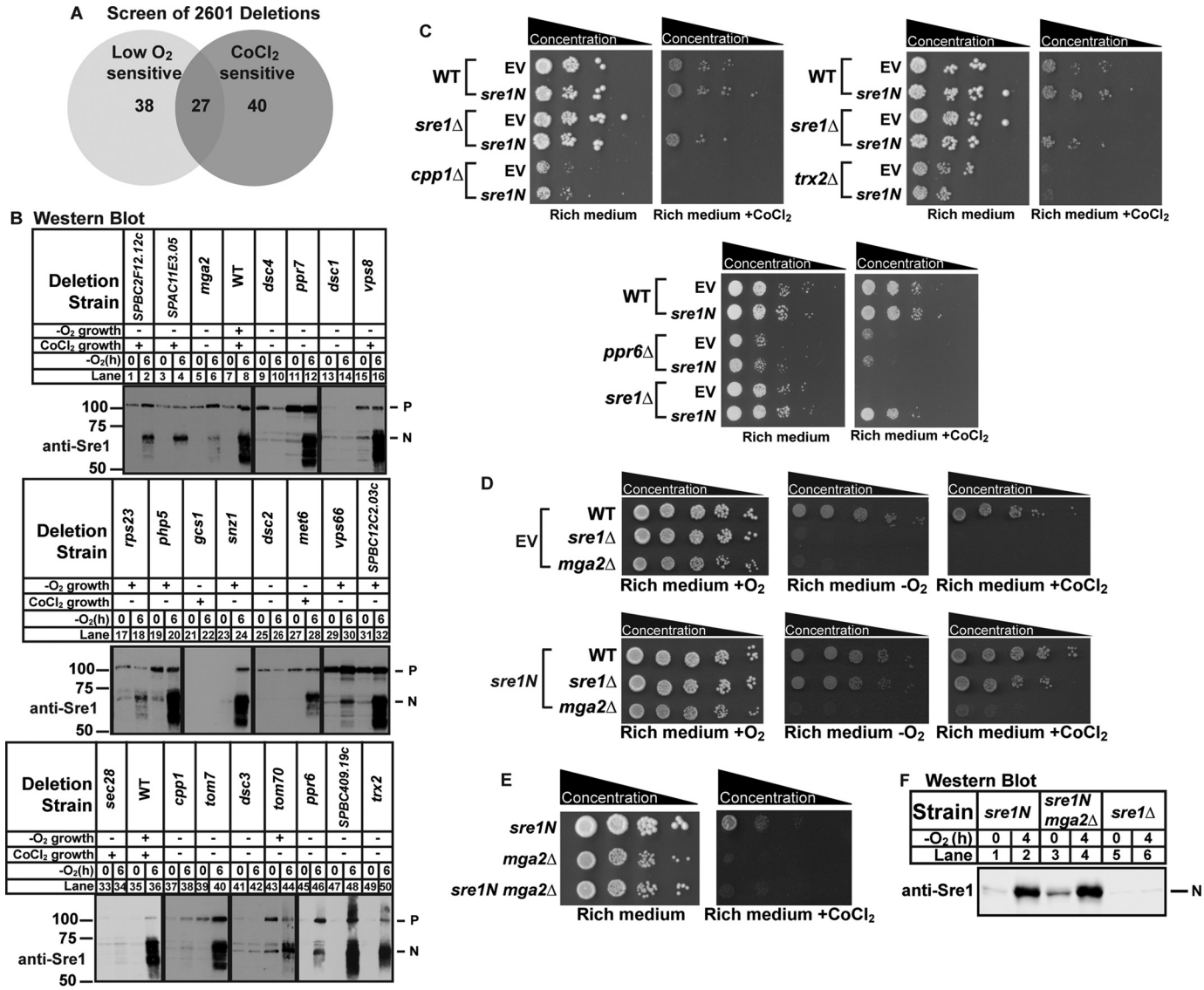

FIGURE 1. **Screen for gene deletions sensitive to low oxygen and cobalt chloride.** *A*, Venn diagram of deletion collection screen results showing overlap between deletions defective for growth under low oxygen and those defective for growth on $CoCl_2$. *B*, Western blots imaged by film probed with anti-Sre1 IgG of lysates from wild-type cells or the indicated deletion strains grown for 0 or 6 h in the absence of oxygen. *P* and *N* denote precursor and cleaved N-terminal transcription factor forms, respectively. Different blots are separated by *solid black lines*. This experiment was performed one time. *C–E*, wild-type or the indicated deletion strains carrying empty vector or a plasmid expressing *sre1N* (*C* and *D*) or with *sre1N* integrated at the endogenous locus (*E*) were grown as indicated for 4 days. Cells were plated in 10-fold serial dilutions ($16–1.6 \times 10^6$ cells). Each experiment was performed with at least two biological replicates. *EV*, empty vector. *F*, indicated strains were grown for 0 or 4 h in the absence of oxygen, and cell lysates were immunoblotted with monoclonal anti-Sre1 5B4 IgG1κ and imaged by Li-Cor. *N* denotes Sre1 N-terminal form. This experiment was performed with three biological replicates.

under low oxygen or on the low oxygen mimetic, $CoCl_2$. Indeed, *sre1*Δ cells fail to grow under both of these conditions (21). To identify genes required for hypoxic adaptation, we screened 2601 mutants from the *S. pombe* non-essential haploid deletion collection for growth in these two conditions. We found that 105 gene deletions were sensitive to low oxygen and/or $CoCl_2$, exhibiting reduced growth in these conditions (Fig. 1*A*). This included 38 deletion mutants sensitive to only low oxygen (1.5% of all tested gene deletions, supplemental Table S2), 40 mutants sensitive to $CoCl_2$ (1.5%, supplemental Table S3), and 27 mutants sensitive to both conditions (1.0%, Table 2). Growth data for the complete screen can be found in supplemental Table S1. Gene ontology term enrichment analysis of deletions sensitive to both low oxygen and $CoCl_2$ (Table 2) showed enrichment for genes involved in "retrograde transport, endosome to Golgi" and the retromer complex ($p < 4E\text{-}3$).

Our previous work identified four of the 27 genes required for growth under low oxygen and on $CoCl_2$ as *dsc1–dsc4*, members of the Dsc E3 ligase complex required for Sre1 cleavage in the Golgi (21). Genes required for Sre1 cleavage fail to accumulate the N-terminal transcription factor (Sre1N) in the absence of oxygen (21). To identify genes functioning in the Sre1 pathway, we assayed low oxygen induction of Sre1N in a number of deletion strains, including the remaining 23 mutants required for growth under low oxygen and on $CoCl_2$ (Fig. 1*B* and Table 2). Immunoblotting against the Sre1 N terminus permits detection of both the full-length precursor form of Sre1 and the transcriptionally active cleaved N terminus. Wild-type cells showed

TABLE 2

Gene deletions sensitive to both hypoxia and cobalt chloride

Strains from the Bioneer haploid deletion collection version 1 found sensitive to both hypoxia and cobalt chloride were tested for rescue of the growth defect by exogenous expression of Sre1 N.

Functional category and systematic ID	Common name	Product[a]	Sre1N production[b]	Rescue with Sre1N[c]
DNA repair				
SPAC13C5.07	*mre11*	Nuclease	+	ND
SPAC644.14c	*rad51*	RecA family recombinase Rad51/Rhp51	+	ND
SPCC338.08	*ctp1*	CtIP-related endonuclease	+	ND
Transcription				
SPAC17G8.05	*med20*	Mediator complex subunit	+	ND
SPBC31F10.09c	*nut2*	Mediator complex subunit Med10	+	ND
SPCC18.06c	*caf1*	CCR4-not complex CAF1 family ribonuclease subunit	+	ND
SPAC26H5.05	*mga2*	IPT/TIG ankyrin repeat containing transcription regulator of FA biosynthesis	−	−
Protein modification				
SPBC947.10	*dsc1*	Golgi Dsc E3 ligase complex subunit	−	+
SPAC1486.02c	*dsc2*	Golgi Dsc E3 ligase complex subunit	−	+
SPAC20H4.02	*dsc3*	Golgi Dsc E3 ligase complex subunit	−	+
SPAC4D7.11	*dsc4*	Golgi Dsc E3 ligase complex subunit	−	+
SPBC4F6.06	*kin1*	Microtubule affinity-regulating kinase	+	ND
SPCC1919.03c	*amk2*	AMP-activated protein kinase β subunit	+	ND
Protein transport				
SPBC409.20c	*psh3*	ER chaperone (SHR3 homolog)	+	ND
Retrograde transport, endosome to Golgi				
SPAC4C5.02c	*ryh1*	GTPase	+	ND
SPAPJ696.01c	*vps17*	Retromer complex subunit	+	ND
SPAC4G9.13c	*vps26*	Retromer complex subunit	+	ND
SPCC777.13	*vps35*	Retromer complex subunit	+	ND
Late endosome to vacuole transport				
SPAC1142.07c	*vps32*	ESCRT III complex subunit	+	ND
Other				
SPBC12D12.07c	*trx2*	Mitochondrial thioredoxin	−	−
SPAC4G8.11c	*atp10*	Mitochondrial F_1-F_0-ATPase assembly protein	+	ND
SPCC306.06c	*big1*	ER membrane protein, BIG1 family	+	ND
SPAC821.05	*tif38*	Translation initiation factor eIF3h	+	−
SPAC17G6.04c	*cpp1*	Protein farnesyltransferase β subunit	−	−
SPBC27B12.10c	*tom7*	Mitochondrial TOM complex subunit	+	ND
SPCC11E10.04	*ppr6*	Mitochondrial PPR repeat protein	−	−
SPBC16A3.03c	*ppr7*	Mitochondrial PPR repeat protein	+	ND

[a] Descriptions were obtained from PomBase with some additional hand editing.
[b] + indicates accumulation of the Sre1N transcription factor to wild type levels.
[c] Rescue of $CoCl_2$ growth defect by Sre1N. + indicates rescue; − indicates no rescue; ND indicates not determined.

robust cleavage and Sre1N production after 6 h at low oxygen (Fig. 1*B*, *lanes 7* and *8*), and four of the deletions sensitive to both low oxygen and $CoCl_2$ (*mga2, cpp1, ppr6,* and *trx2*) showed reduced Sre1N accumulation (Fig. 1*B* and Table 2). These deletions represent new candidates for genes required for Sre1 activation in *S. pombe*. The remaining 19 deletions showed normal Sre1N accumulation (Table 2) and thus are genes that could be involved in low oxygen-responsive pathways distinct from Sre1 target gene transcription.

To test whether a failure to produce Sre1N caused the observed growth defects in the absence of these four genes (*mga2, cpp1, ppr6*, and *trx2*), we expressed *sre1N* from a plasmid and assayed growth on $CoCl_2$. Notably, none of these deletion strains was rescued by *sre1N* expression (Fig. 1, *C* and *D*), suggesting that either the Sre1N production defect occurs after cleavage (*e.g.* Sre1N is highly unstable) or that the deletion mutant is $CoCl_2$-sensitive for reasons unrelated to Sre1N function.

Of the four genes, we focused our studies on *mga2* because Mga2 is a putative transcriptional activator in fission yeast based on homology to two related transcriptional activators in *S. cerevisiae*, *MGA2,* and *SPT23* (18). Therefore, Mga2 was a candidate for a new regulator of a low oxygen response. To confirm that the defect in growth of *mga2*Δ cells on cobalt chloride was not due to the observed Sre1 cleavage defect, we expressed the *sre1N* transcription factor from the endogenous *sre1* locus and assayed transcription factor activity and growth on $CoCl_2$. As with the plasmid-based *sre1N* previously examined, expression of *sre1N* from the endogenous locus did not rescue $CoCl_2$ growth of *mga2*Δ cells (Fig. 1*E*). Importantly, full activation of Sre1 production under low oxygen requires positive feedback regulation in which Sre1 stimulates *sre1* transcription (28). In the absence of *mga2,* Sre1N up-regulated its own expression under low oxygen through positive feedback to wild-type levels (Fig. 1*F*). These data suggest the following: 1) that *mga2*Δ cells are defective for proteolytic activation of Sre1 precursor, rather than at a step downstream of cleavage, and 2) that the Sre1 cleavage defect cannot fully account for the observed growth defects of *mga2*Δ cells on $CoCl_2$. Based on our interest in the hypoxic transcriptional response and the known function of *S. cerevisiae mga2* homologs as transcriptional activators, we further analyzed the requirement for *mga2* in fission yeast low oxygen adaptation.

Cell Growth Requires Mga2 in the Presence and Absence of Oxygen—To characterize the requirement for *mga2* in response to changes in environmental oxygen, we measured

growth in liquid culture of wild-type and *mga2*Δ cells in either the presence or absence of oxygen. *mga2*Δ cells showed significantly reduced growth compared with wild-type cells in both conditions and further reduced growth in the absence of oxygen compared with the presence of oxygen (Fig. 2*A*). Consistent with the observation that functional Sre1N transcription factor does not rescue $CoCl_2$ growth in the absence of *mga2* (Fig. 1, *E* and *F*), Sre1N did not rescue either the plus oxygen or minus oxygen liquid growth defects (Fig. 2*B*). Given that *sre1*Δ cells exhibit wild-type growth in the presence of oxygen (9), these growth assays demonstrate that *mga2* functions in adaptation to low oxygen and $CoCl_2$ through Sre1-independent pathway(s).

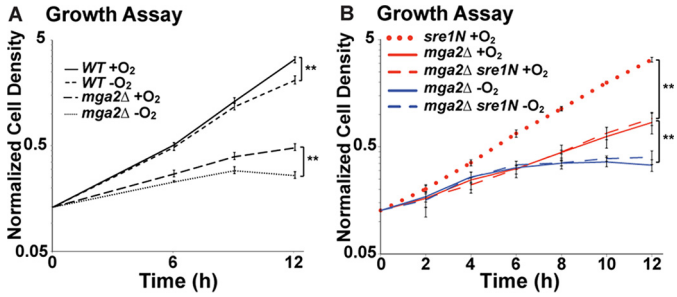

FIGURE 2. **Sre1N does not rescue *mga2*Δ growth defect.** Indicated strains were grown in liquid culture in the presence or absence of oxygen for 12 h. Cell density was measured by absorbance at 600 nm. Data points are average of three biological replicates. *Error bars* are 1 S.D. (**, $p < 0.01$ by two-tailed Student's *t* test for 12-h time point). *A*, absorbance at time 0 among the samples ranged from 0.13 to 0.18. To focus on the difference in growth rate among conditions, we normalized the data for each sample to a value of 0.15 at time point 0 before averaging. *B*, absorbance at time 0 among the samples ranged from 0.09 to 0.16. To focus on the difference in growth rate among the six conditions, we normalized the data for each sample to a value of 0.13 at time point 0 before averaging.

Mga2 Functions as a Transcriptional Regulator of Lipid Metabolism—Uncharacterized in *S. pombe*, *mga2* is the sole fission yeast homolog of *S. cerevisiae MGA2* and *SPT23*. *S. cerevisiae MGA2*, but not *SPT23*, is required for low oxygen induction of transcription of the Δ9 fatty acid desaturase *OLE1* and modulates the stability of *OLE1* mRNA in response to fatty acid availability (19, 29). *S. cerevisiae* Mga2 also up-regulates transcription of other genes involved in fatty acid and sterol homeostasis under oxidative stress, including *ERG1, FAS1, ELO1, FAA4,* and *ATF1* (30). Although a combined deletion of both *MGA2* and *SPT23* in *S. cerevisiae* is lethal, deletion of *mga2* in *S. pombe* was slow growing but viable under normoxia (Figs. 1*D* and 2*A*). The low oxygen sensitivity of the *mga2*Δ mutant led us to investigate Mga2-dependent transcription in *S. pombe* under low oxygen.

To determine the transcriptional targets of *S. pombe* Mga2, we performed genome-wide expression profiling under low oxygen. We compared gene expression in *sre1*Δ cells to *sre1*Δ *mga2*Δ cells after 1.5 h of growth in the absence of oxygen. We deleted *sre1* in both strains so that observed changes in gene expression would be due to loss of *mga2* and not indirect effects of the Sre1 cleavage block that occurs in *mga2*Δ cells (Fig. 1*B*). Of the 5057 genes examined, 291 (5.8%) were significantly decreased in *mga2*Δ cells by SAM. The full list of Mga2-dependent genes can be found in supplemental Tables S4 and S5. Gene ontology term enrichment analysis of the decreased genes identified fatty acid metabolism and lipid metabolism as affected pathways (p value <0.0001). Table 3 lists genes that decreased expression at least two standard deviations from the mean in *mga2*Δ cells. These included long-chain fatty acid CoA ligases (*lcf1* and *lcf2*), TAG lipases (*ptl1* and *ptl2*), and the Δ9

TABLE 3

mga2Δ transcriptional targets hypoxic microarray

Functional category and systematic ID[a]	Common name	*S. cerevisiae* homolog[b]	Product[b]	log2 fold change,[c] WT/*mga2*Δ	Sre1 target[d]
Lipid metabolism					
SPAC1B3.16c	*vht1*	*VHT1*	Biotin transporter	2.69	−
SPBC18H10.02	*lcf1*	*FAA1,FAA3,FAA4*	Long-chain fatty-acid-CoA ligase	2.66	−
SPCC1450.16c	*ptl1*	*TGL3*	Triacylglycerol lipase	2.57	−
SPAC1786.01c	*ptl2*	*TGL4,TGL5*	Triacylglycerol lipase	2.32	−
SPAC30D11.11		*IZH3*	Hemolysin-III family protein (homolog to adipo-Q receptor)	2.31	−
SPAC589.09	*csr101*	*CSR1*	sec14 cytosolic factor family, glycerophospholipid transfer protein	1.69	+
SPBP4H10.11c	*lcf2*	*FAA1,FAA3,FAA4*	Long-chain fatty acid-CoA ligase	1.79	+
SPCC1281.06c	*ole1*	*OLE1*	Acyl-CoA desaturase, ole1	1.74	−
SPCC1235.02	*bio2*	*BIO2*	Biotin synthase	1.68	−
SPAC2F3.09	*hem1*	*HEM1*	5-Aminolevulinate synthase	1.63	−
SPAC4A8.10	*rog1*	*ROG1*	Acylglycerol lipase	1.62	−
SPAC22A12.06c	*fsh2*	*FSH2*	Serine hydrolase-like protein	1.61	+
SPBC646.07c	*tsc13*	*TSC13*	Enoyl reductase (predicted)	1.60	−
SPAC56E4.04c	*cut6*	*ACC1,HFA1*	Acetyl-CoA/biotin carboxylase	1.58	−
Other					
SPBC1778.04	*spo6*	*DBF4*	Spo4-Spo6 kinase complex regulatory subunit	3.19	−
SPBC359.04c	*pfl7*		Cell surface glycoprotein, DIPSY family	3.05	−
SPAC3G6.05		*YOR292C*	Mpv17/PMP22 family protein 1	2.27	−
SPBC359.02	*alr2*		Alanine racemase	2.18	−
Unknown					
SPAC17A2.02c		*TDA4*	DUF887 family protein	2.01	−
SPAC5H10.07			Sequence orphan	1.54	−
SPCP20C8.03			Pseudogene	1.51	−
SPCC1281.08	*wtf11*		wtf element Wtf11	1.50	−

[a] Genes showing anaerobic induction in Todd *et al.* (9) are underlined.
[b] Descriptions and homologs were obtained from PomBase with some additional hand editing.
[c] Data are presented as the average changes in expression of genes in *sre1*Δ (WT) samples after 1.5 h without O_2 compared with the expression of genes in *sre1*Δ*mga2*Δ (*mga2*Δ) samples after 1.5-h without O_2. For clarity, only data greater than 2 S.D. from the average fold change are presented in this table. Full results are detailed in supplemental Tables S4 and S5.
[d] Statistically significant target assignment from low oxygen microarray was from Todd *et al.* (9).

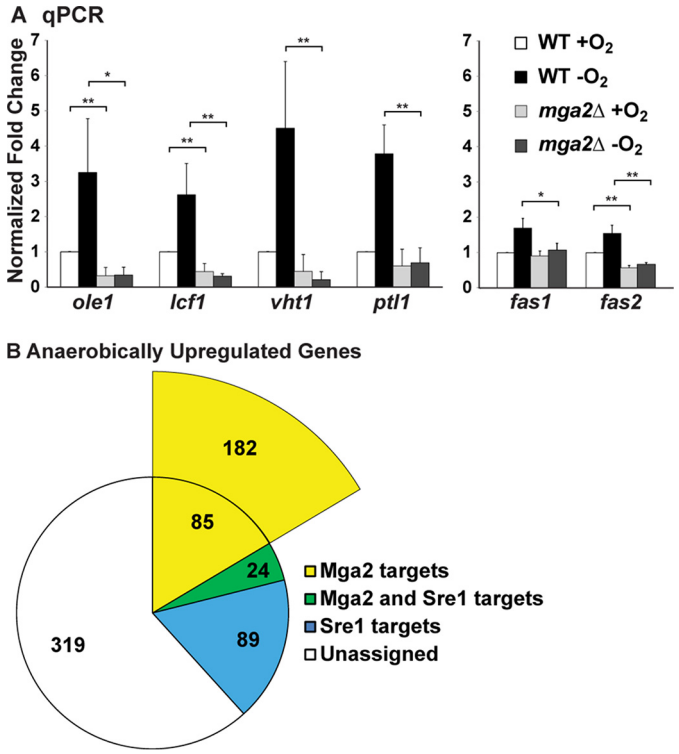

FIGURE 3. **Mga2 controls low oxygen gene expression.** *A*, wild-type and *mga2*Δ cells were grown for 4 h in the presence or absence of oxygen. qPCR analysis was performed for the indicated genes. *Error bars* are standard deviation of five biological replicates. Two technical replicates were performed per sample. *, p value < 0.05; **, p value < 0.005 by two-tailed Student's t test. The two *graphs* represent two independently performed sets of experiments. *B*, *pie chart* comparing gene populations from different data sets: anaerobically up-regulated genes from Todd *et al.* (9) reside in the *circle*; *blue,* Sre1 targets from Todd *et al.* (9); *yellow*, Mga2 targets from this study (supplemental Table S5); *green,* targets of both Sre1 and Mga2; *white,* targets of neither Sre1 or Mga2. Mga2 targets that are not anaerobically up-regulated are represented in a *wedge* outside of the *circle*.

fatty acid desaturase (*ole1*). Additionally, Mga2 controls expression of the biotin transporter *vht1* and biotin synthase *bio2*, as well as *hem1*. Biotin is required for acetyl-CoA carboxylase function, and heme is a prosthetic group for Ole1 in *S. cerevisiae* (31). Although transcriptome profiling for *S. cerevisiae MGA2*-dependent genes under low oxygen conditions has not been performed, homologs of known *S. cerevisiae* Mga2-dependent genes were decreased in our *mga2*Δ cells (Table 3 and supplemental Table S5). Our microarray results suggest that fission yeast Mga2 regulates many lipid metabolism genes.

To confirm the microarray results, we assayed low oxygen expression of candidate Mga2 target genes in wild-type and *mga2*Δ cells by quantitative real time PCR. Expression of *ole1*, *lcf1*, *vht1*, *ptl1*, *fas1*, and *fas2* increased in the absence of oxygen, and this induction required *mga2* (Fig. 3*A*). Expression of *ole1, lcf1*, and *fas2* was also reduced even in the presence of oxygen, indicating that *mga2* is required for gene expression both in the presence and absence of oxygen.

To assess the oxygen regulation of all Mga2 targets, we compared our microarray results with known data sets. A previous study in our laboratory identified *S. pombe* genes up-regulated after 1.5 h of low oxygen treatment (9). 37% of Mga2 target genes were up-regulated under low oxygen in that study (Fig. 3*B* and supplemental Table S5). This accounts for 21% of all low oxygen up-regulated genes (9). If we consider those genes most dependent on Mga2 (those showing expression reduced more than 2 S.D. from the mean in the absence of *mga2*), 68% of these genes were up-regulated under low oxygen in our previous study (Table 3, underlined IDs). Only 21% of Sre1 target genes were also regulated by Mga2 under low oxygen, confirming that Mga2 promotes a low oxygen-responsive pathway that is distinct from the Sre1 pathway (Tables 3, supplemental Table S5, and Fig. 3*B*) (9). We conclude that *S. pombe* Mga2 regulates lipid metabolism gene expression in the presence of oxygen and that there is an additional requirement when oxygen is limiting.

Maintenance of Lipid Homeostasis Requires Mga2—We hypothesized that failure to up-regulate genes involved in lipid biosynthesis in *mga2*Δ cells may lead to alterations in lipid homeostasis. To measure levels of cellular lipids, we performed quantitative mass spectrometry-based lipidomics on wild-type and *mga2*Δ cells grown in the presence of oxygen (23). We examined cells in the presence of oxygen because oxygen is required for fatty acid desaturation and ergosterol synthesis (32–34), so the absence of oxygen would alter lipid synthesis regardless of strain background. Additionally, Mga2 target genes showed reduced expression in *mga2*Δ cells in the presence of oxygen (Fig. 3*A*). Full data and data analysis of this lipidomics experiment can be found in supplemental Table S6.

Our lipidomics experiment showed that in *mga2*Δ cells, diacylglycerol and TAG levels decreased, whereas glycerophospholipid levels varied, with PA and PE increasing, phosphatidylinositol decreasing, and phosphatidylserine and cardolipin levels unchanged (Fig. 4*A*). Interestingly, these alterations in glycerophospholipids were largely not reflected in the lysophospholipids that are inputs and products of glycerophospholipids. Lysophosphatidylcholine and lysophosphatidylethanolamine levels decreased, despite the fact that phosphatidylcholine was unchanged and PE levels were higher in *mga2*Δ cells (Fig. 4*A*). Although levels of both ceramide and mannosylinositol phosphorylceramide were unchanged, levels of the intermediate inositol phosphorylceramide increased in the absence of *mga2* (Fig. 4*A*). Levels of ergosterol increased in *mga2*Δ cells, whereas lanosterol decreased (supplemental Table S6).

In the absence of *mga2*, glycerophospholipids decreased in chain length, especially in phosphatidylcholine, PA, and PE, although phosphatidylinositol chain lengths increased slightly (Fig. 4*B*). No significant changes occurred in lysophospholipid chain length (supplemental Table S6). Decreased acetyl-CoA carboxylase *cut6* and enoyl reductase *tcs13* expression (Table 3) may play a role in the observed decreases in fatty acid chain length. Taken together, these data demonstrate widespread lipidome disruption in the absence of *mga2* and thus position this transcriptional activator as a crucial regulator of TAG and glycerophospholipid homeostasis.

Glycerophospholipid Saturation Increases in the Absence of Mga2—MGA2 and *SPT23*, the *S. cerevisiae* homologs of *mga2,* regulate the Δ9 fatty acid desaturase *OLE1* required for fatty acid desaturation. Notably, Mga2 in fission yeast also regulated the Δ9 fatty acid desaturase *ole1* (Fig. 3*A*). To determine whether decreased expression of *ole1* resulted in altered glycerophospholipid saturation in *mga2*Δ cells, we examined fatty acid saturation in our lipidomics experiment. All glycerophos-

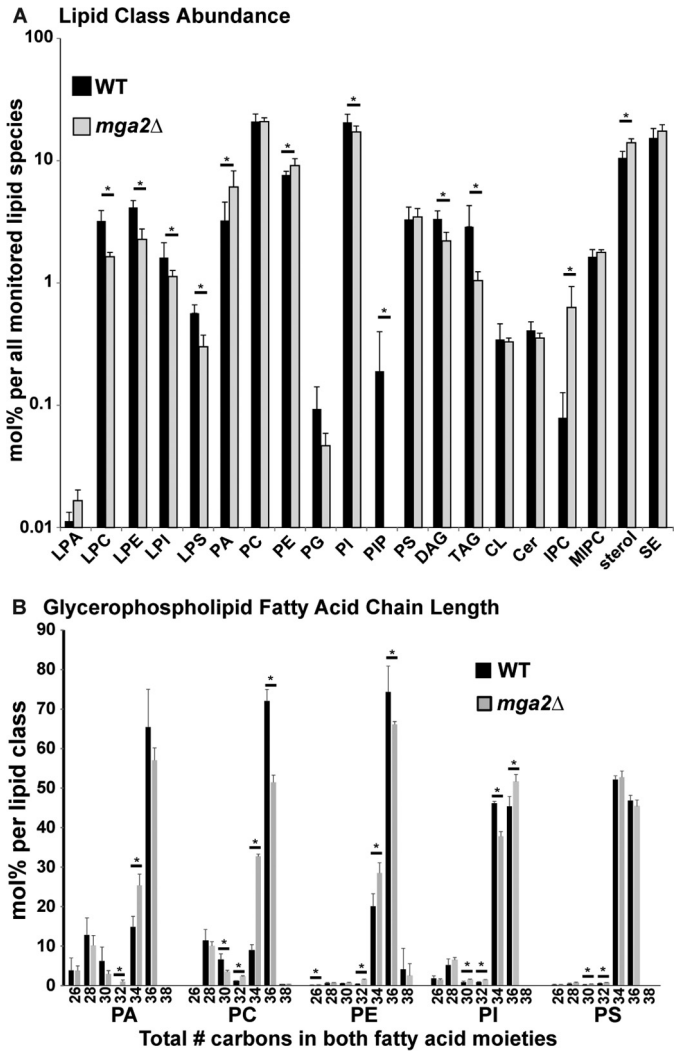

FIGURE 4. **Mga2 regulates lipid homeostasis.** Wild-type or *mga2*Δ cells were grown to exponential phase in liquid culture in the presence of oxygen. High resolution shotgun lipidomics was performed on six biological replicates (two technical replicates) to quantify the abundances of lipid species in the *S. pombe* lipidome. Full results are available in supplemental Table S6. *Error bars* represent 1 S.D. *p* values were calculated using a two-tailed Mann-Whitney *U* test and corrected for multiple comparisons using Benjamini and Hochberg's method to produce a false discovery rate, *q*. *, *q* value <0.05. *LPA*, lysophosphatidic acid; *LPC*, lysophosphatidylcholine; *LPE*, lysophosphatidylethanolamine; *LPI*, lysophosphatidylinositol; *LPS*, lipopolysaccharide; *PA*, phosphatidic acid; *PC*, phosphatidylcholine; *PE*, phosphatidylethanolamine; *PG*, phosphatidylglycerol; *PI*, phosphatidylinositol; *PIP*, phosphoinositol phosphate; *PS*, phosphatidylserine; *DAG*, diacylglycerol; *TAG*, triacylglycerol; *CL*, cardolipin; *Cer*, ceramide; *IPC*, inositol phosphorylceramide; *MIPC*, mannosylinositol phosphorylceramide.

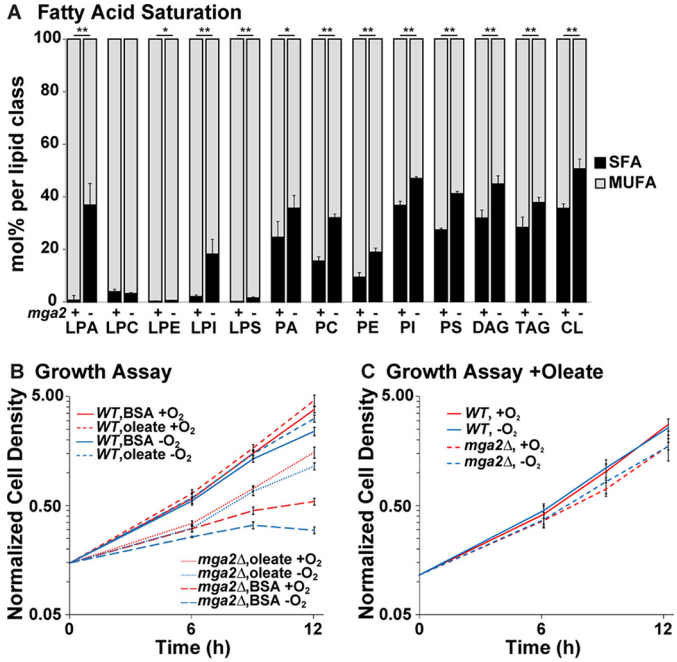

FIGURE 5. **Unsaturated fatty acids rescue *mga2*Δ growth defect.** *A*, saturation of fatty acyl chains in wild-type and *mga2*Δ cells. Saturation of each chain was determined rather than the saturation of a lipid species as a whole (see "Experimental Procedures"). *SFA* is saturated fatty acids, and *MUFA* is monounsaturated fatty acids. *Error bars* are 1 S.D. *p* values were calculated using a two-tailed Mann-Whitney *U* test and corrected for multiple comparisons using Benjamini and Hochberg's method to produce a false discovery rate, *q*. *, *q* value <0.05; **, *q* value <0.01. *B* and *C*, wild-type and *mga2*Δ cells were grown for 12 h in the presence (*red*) or absence (*blue*) of oxygen, with the addition of BSA alone or oleic acid (18:1) conjugated to BSA. Cell density was measured by absorbance at 600 nm. Data points are average of three biological replicates. *Error bars* are 1 S.D. *B*, BSA alone or oleic acid (18:1) was added at time 0. Absorbance at time 0 among the samples ranged from 0.13 to 0.18. To focus on the difference in growth rate among the conditions, we normalized the data for each sample to a value of 0.15 at time point 0 before averaging. The BSA only data are identical to those in Fig. 2*A*. *C*, oleic acid (18:1) was added 16 h prior to time 0 and then cells were diluted into fresh oleic acid medium at time 0. Absorbance at time 0 among the samples ranged from 0.09 to 0.14. To focus on the difference in growth rate among the conditions, we normalized the data for each sample to a value of 0.12 at time point 0 before averaging. *LPA*, lysophosphatidic acid; *LPC*, lysophosphatidylcholine; *LPE*, lysophosphatidylethanolamine; *LPI*, lysophosphatidylinositol; *LPS*, lipopolysaccharide; *PA*, phosphatidic acid; *PC*, phosphatidylcholine; *PE*, phosphatidylethanolamine; *PI*, phosphatidylinositol; *PS*, phosphatidylserine; *DAG*, diacylglycerol; *TAG*, triacylglycerol; *CL*, cardolipin.

pholipids measured, as well as lysophosphatidic acid, lysophosphatidylinositol, lysophosphatidylethanolamine, LPS, diacylglycerol, and TAG showed increased saturation in *mga2*Δ cells (Fig. 5*A*). Together, these data suggest that even in the presence of oxygen, *mga2*Δ cells exhibit strongly decreased levels of lipid molecules with unsaturated fatty acid moieties.

To test whether the observed plus and minus oxygen growth defects resulted from reduced fatty acid desaturation, we grew wild-type and *mga2*Δ cells in liquid medium supplemented with monounsaturated oleic acid (18:1) conjugated to BSA (oleic acid) or with BSA alone. Oleic acid is the most abundant unsaturated fatty acid in fission yeast, representing about 75% of all fatty acids in the cell (35). Oleic acid or BSA was added to the media at the 0-h time point, and cell density was measured for the following 12 h. Oleic acid addition had no effect on growth of wild-type cells but rescued growth of *mga2*Δ cells in both the presence and absence of oxygen (Fig. 5*B*).

Although the oleic acid-treated *mga2*Δ cells did not reach a density equal to that of wild type after 12 h, calculation of the cellular growth rates showed rescue. Oleic acid-treated *mga2*Δ cells exhibited a doubling time similar to that of BSA-treated *mga2*Δ cells during the first 6 h of treatment, but they grew like wild-type cells during the second 6 h of treatment (Table 4). These data suggest that normal growth of *mga2*Δ cells requires a lag phase, perhaps to allow oleic acid uptake and incorporation into cellular lipids.

To test this hypothesis, we grew wild-type and *mga2*Δ cells under normoxia for 16 h plus oleic acid, then diluted the cells into fresh oleic acid-containing medium, and grew the cells in

TABLE 4

Doubling time of *WT* and *mga2*Δ cells after oleate addition

Table shows the doubling times for growth curves in Fig. 5*B*. Cells were grown in BSA/oleate or BSA alone for 12 h ± oxygen. Doubling times were calculated using 0- and 6-h or 6- and 12-h optical density readings as indicated, using the formula: doubling time = (culture time × log(2))/log(final OD) − log(initial OD). Doubling times are displayed as mean ± S.D. for three biological replicates.

		0–6 h		6–12 h	
Strain	Oxygen	−Oleate	+Oleate	−Oleate	+Oleate
WT	+	3.1 ± 0.1	2.9 ± 0.2	2.2 ± 0.1	2.1 ± 0.0
WT	−	3.2 ± 0.2	3.1 ± 0.3	2.9 ± 0.0	2.5 ± 0.1
*mga2*Δ	+	5.8 ± 0.6	5.1 ± 0.4	7.3 ± 0.5	2.8 ± 0.1
*mga2*Δ	−	7.6 ± 0.2	5.8 ± 0.6	39.2 ± 29.3	3.2 ± 0.0

TABLE 5

Doubling time of *WT* and *mga2*Δ cells after oleate preincubation

Table shows the doubling times for growth curves in Fig. 5*C*. Cells were grown for 16 h in BSA/oleate under normoxia and then in BSA/oleate for 12 h ± oxygen. Doubling times were calculated using 0- and 12-h optical density readings as indicated, using the formula doubling time = (culture time × log(2))/log(final OD) − log(initial OD). Doubling times are displayed as mean ± S.D. for three biological replicates.

Strain	Oxygen	d*t*
		h
WT	+	2.6 ± 0.1
WT	−	2.7 ± 0.2
*mga2*Δ	+	3.1 ± 0.1
*mga2*Δ	−	3.1 ± 0.3

the presence or absence of oxygen for another 12 h (Fig. 5*C*). As expected, preincubation of *mga2*Δ cells with oleic acid eliminated the lag phase and *mga2*Δ cells showed wild-type growth from the 0-h time point (Fig. 5*C* and Table 5). Therefore, we conclude that addition of exogenous oleic acid fully rescues growth defects of *mga2*Δ cells both in the presence and absence of oxygen.

Discussion

This study represents the first screen of the *S. pombe* nonessential haploid deletion collection version 1.0 for gene deletions sensitive to low oxygen. We identified 105 gene deletions that resulted in sensitivity to low oxygen and/or the low oxygen mimetic $CoCl_2$, with 27 deletions resulting in sensitivity to both. Interestingly, we identified 19 genes that are required for adaptation to low oxygen stress but are not deficient in Sre1N accumulation (Table 2). These genes may represent other pathways required to adapt to oxygen stress, or they may regulate Sre1 signaling at a post-cleavage step, such as regulating Sre1 binding to promoters. These genes include multiple players of three separate pathways (supplemental Tables S2 and S3).

The first highly represented pathway sensitive to low oxygen and $CoCl_2$ is transport between the endosome and the Golgi or the vacuole (*ryh1, sec28, vsp8, vps17, vps24, vps26, vps29, vps32, vps35,* and *vps36*). This transport could be required to maintain V-type H^+-ATPase at the vacuole. It has been shown in budding yeast that in the absence of V-ATPase function, the cytosol acidifies (36). Normally, the plasma membrane proton pump Pma1 would compensate by hydrolyzing ATP and pumping out protons (37). However, under low oxygen, reduced oxidative respiration may decrease cellular ATP (38), creating conditions that require full V-ATPase activity to maintain cytosolic pH.

The second pathway sensitive to both low oxygen and $CoCl_2$ is Mediator (*med20* and *nut2*). Highly conserved from yeast to humans, the Mediator complex, composed of 13 subunits in fission yeast, is required for regulated expression of most RNA polymerase II-dependent genes (39, 40). A potential role of Mediator in regulating low oxygen adaptation in fission yeast is consistent with data in humans and *Caenorhabditis elegans* showing that Mediator is required for SREBP transcriptional activation of target genes, as well as lipid homeostasis and fatty acid desaturation (41). Because mediator is required at a post-cleavage step in the SREBP pathway, the effects of these mutants may not be apparent in a cleavage assay.

A third pathway sensitive to only low oxygen in our screen is miRNA biogenesis (*arb1, arb2,* and *dcr1*). Interestingly, a number of recent papers have suggested that chronic hypoxia induces down-regulation of miRNA biogenesis to maintain hypoxia-inducible factor-α (HIFα) induction in vascular endothelial and cancer cell lines (42–44). This adaptation is correlated with tumor progression and poor prognosis (43, 44). However, other recent work has identified the micro-RNA miR-210 as a "master" hypoxia-regulated miRNA, exhibiting up-regulation by HIF-1α under conditions of hypoxia (45–47). miR-210 promotes cell cycle progression and evasion of apoptosis while compromising mitochondrial integrity and DNA repair in numerous cancer cell lines (47). Additional work is required to fully understand the complex interplay between miRNA biogenesis and hypoxia adaptation in human cells, as well as in fission yeast, which lack an HIF homolog.

In addition to *mga2*, this screen identified three genes that were required for Sre1N accumulation but were not rescued by exogenous Sre1N (Fig. 1*C*). Cpp1 is a subunit of protein farnesyltransferase required for farnesylation of small GTPases such as Ras and Rheb. *cpp1*Δ exhibits severe normoxia growth defects and temperature sensitivity as well as morphological defects, indicating a role for farnesylation in a number of processes, one of which may be Sre1 activation (48). Trx2 is a mitochondrial oxidoreductase that helps to maintain the mitochondrial redox state, especially in the absence of glutathione (49, 50). Ppr6 is a mitochondrial membrane protein that regulates the mRNA stability of the mitochondrial ATP synthase subunit *atp9*. In the absence of *ppr6*, *atp9* mRNA is reduced, and cells become sensitive to galactose and antimycin, indicating defects in aerobic respiration (51). Taken together, these data suggest a role for mitochondrial function in regulating Sre1 activation and cellular adaptation to low oxygen and $CoCl_2$.

Ryuko *et al.* (52) previously performed a screen of the 3004 *S. pombe* deletion collection version 2.0 strains for growth on 3.5 mM $CoCl_2$. We used 1.6 mM $CoCl_2$ in our screen. They found 54 gene deletions sensitive to $CoCl_2$ and 56 gene deletions resistant to $CoCl_2$. Of the 67 deletions that we found sensitive to $CoCl_2$, only 11 were also identified by Ryuko *et al.* (52) as sensitive to $CoCl_2$ (supplemental Table S3). The small overlap between these studies may be due to the different concentrations of $CoCl_2$ used, leading to selection for different responses to the chemical. We chose a concentration sufficient to inhibit growth of *sre1*Δ cells to mimic hypoxia. By screening under two conditions (low oxygen and $CoCl_2$), we focused our search to those genes most likely to be involved in low oxygen response. Additionally, another group recently screened the 669 strains of deletion collection version 2.0 that are not present in deletion

collection version 1.0 (screened in this study) for growth on both $CoCl_2$ and under low oxygen conditions. They identified 33 genes required for growth under low oxygen and/or $CoCl_2$ conditions, although they only reported the identity of one, the rhomboid protease *rbd2* (53).

We focused our studies on the transcriptional activator Mga2, which our screen showed is required for low oxygen adaptation (Fig. 1*D*). Multiple lines of evidence support the conclusion that Mga2 regulates an oxygen-responsive transcriptional program that is independent from the Sre1 pathway. First, transcriptionally active Sre1N did not rescue low oxygen and $CoCl_2$ growth of *mga2*Δ cells (Figs. 1, *E* and *F*, 2*B*). Second, *mga2*Δ cells exhibited a growth defect in the presence of oxygen, whereas *sre1*Δ cells have no normoxia growth defects (Fig. 2*A*) (8). Third, Mga2 regulates numerous genes not known to be oxygen-dependent, whereas Sre1 activity is only required under low oxygen (Fig. 3, *A* and *B*, and supplemental Table S5) (9). Finally, comparison of our list of Mga2 low oxygen gene expression targets with the known list of Sre1 expression targets showed only 22% overlap (most notably *csr101, lcf2, fsh2,* and *hmg1*) (Table 3 and Fig. 3*B*). Instead, Mga2 regulated genes primarily involved in TAG and glycerophospholipid homeostasis, including the fatty-acid synthases *fas1* and *fas2*, the fatty acid desaturase *ole1*, and the long chain fatty acid CoA ligase *lcf1* (Table 3 and Fig. 3*A*). This study positions Mga2 at the head of a new oxygen-responsive pathway in fission yeast.

Although Sre1 is regarded as the SREBP-2 analog that regulates sterol synthesis in *S. pombe*, no SREBP-1 analog regulating TAG and glycerophospholipid synthesis has been described. Given the results described in this study, we propose that *mga2* is the SREBP-1 analog in fission yeast. Indeed, the list of Mga2 gene targets is strikingly similar to the known gene targets of mammalian SREBP-1 (8/9 targets conserved, supplemental Table S5) (4, 54). Therefore, we conclude that Mga2 serves as the analogous transcription factor to SREBP-1 in *S. pombe* by coordinately regulating TAG and glycerophospholipid metabolism. Importantly, only 38% of *S. pombe* anaerobically up-regulated genes are transcriptional targets of either Mga2 or Sre1 (Fig. 3*B*). Thus, additional transcriptional regulators of low oxygen-responsive pathways, including carbohydrate synthesis and the mitochondrial response, remain to be discovered (9).

Although this study is the first characterizing the transcriptional regulation of glycerophospholipid and TAG metabolism in fission yeast, glycerolipid regulation is much better characterized in *S. cerevisiae*. There, PA signals the glycerolipid state of the cell, as all membrane phospholipids and TAG are synthesized from PA. Low levels of membrane PA cause the Opi1 repressor to leave the perinuclear ER membrane and enter the nucleus. There it represses phospholipid synthesis genes to maintain lipid homeostasis (55). Interestingly, there is no known Opi1 homolog in *S. pombe*, raising the question as to whether a different method is used to sense PA availability. Given the high degree of functional conservation between fission yeast and mammals, studies of phospholipid homeostasis in fission yeast may provide insight into the regulation of this pathway in mammals.

Interestingly, a recent report suggested that the CSL transcription factor Cbf11 binds to the promoters of seven Mga2 target genes in *S. pombe* (56). Although *cbf11* is not itself an Mga2 target gene (supplemental Table S4), deletion of *cbf11* results in a low oxygen growth defect in our screen (supplemental Tables S1 and S2), and Cbf11 was found to bind Mga2 in an affinity capture screen for the fission yeast protein interactome network (57). The Cbf11 human homologs RBPJ and RBPJL share ~19% protein sequence identity with Cbf11 (clustered in the functional domains), raising the possibility that these proteins perform similar functions. These RBP family transcription factors mediate Notch signaling and are required for pancreas development (58, 59). It is intriguing to speculate that fission yeast Mga2 and Cbf11 may act together to regulate phospholipid and TAG metabolism in response to low oxygen. More work is required to determine whether and how these two transcription factors work together to regulate lipid homeostasis.

These results support a model for *S. pombe* low oxygen lipid homeostasis in which decreased oxygen availability results in reduced ergosterol synthesis. This activates Sre1, increasing expression of enzymes required for ergosterol synthesis and restoring homeostasis (8). At the same time, low oxygen availability also results in reduced fatty acid desaturation. This activates Mga2, increasing expression of *ole1* and up-regulating unsaturated fatty acid synthesis. Interestingly, although both SREBP-1 and SREBP-2 are activated by the same machinery in mammalian cells, Sre1 and Mga2 are not processed coordinately (60). Instead, Sre1 is activated through the function of a Golgi-resident Dsc E3 ligase and a rhomboid protease, whereas *S. cerevisiae* Mga2 and Spt23 are activated by the Rsp5 ubiquitin ligase and the proteasome (21, 53, 61). Independent activation of Sre1 and Mga2 is supported by the fact that cells lacking a Dsc E3 ligase component show wild-type normoxic growth unlike *mga2*Δ cells, indicating that the Dsc E3 ligase is not required for Mga2 activation (data not shown).

Despite differing mechanisms of regulation, both of these pathways are likely product inhibited. Work in mammalian cells has shown that SREBP trafficking by Scap is inhibited by exogenous cholesterol, although the parallel experiment cannot be performed in *S. pombe* as fission yeast do not uptake ergosterol (8, 62, 63). Similarly, work in *S. cerevisiae* showed a block in Mga2 activation when exogenous unsaturated fatty acid was added to the medium (61). Consistent with this result, activation of SREBP-1, but not SREBP-2, is inhibited by addition of exogenous arachidonate (20:4) in HEK293 cells (64). Because both ergosterol and unsaturated fatty acids require oxygen for synthesis, product inhibition of these two pathways would allow indirect sensing of oxygen availability. Additionally, as membrane production requires coordinated supply of both ergosterol and glycerophospholipids, cross-talk between these two pathways is likely. Future studies will examine coordination of these two oxygen-responsive pathways.

An important next step will be to examine whether unsaturated fatty acids regulate Mga2 through protein levels or activation. Alternatively, there could be other modes of regulation of these genes by oxygen. Our observation that Mga2 activates genes under normoxia and that expression is further increased under low oxygen conditions (Fig. 3*A*) suggests that there may be constitutive activation of Mga2 under all oxygen conditions

and that an additional oxygen-responsive transcription factor may cooperate with Mga2 under low oxygen.

Finally, the Mga2 pathway represents a new avenue for antifungal drug discovery. Recent reports have shown that pathogenic fungi must adapt to the low oxygen environment of the host tissue to cause disease (15–17, 65). Importantly, *mga2* has apparent homologs in multiple pathogenic fungi, including *Aspergillus fumigatus, Aspergillus flavus, Histoplasma capsulatum, Cryptococcus neoformans, Cryptococcus gattii, Candida albicans,* and *Candida glabrata.* These homologs are characterized by an IPT (Ig-like, plexins, transcription factors) transcription factor immunoglobulin-like DNA binding domain, an ankyrin repeat, and a transmembrane domain near the C terminus (66, 67). Many of these pathogenic fungi also have SREBP homologs, suggesting overall conservation of these parallel oxygen-adaptation pathways (15, 17). Additionally, unlike the SREBP transcription factors, Mga2 has no apparent homologs in humans, limiting the potential toxic effects of drugs targeting this pathway. Future studies will characterize *mga2* homologs in these organisms to determine whether they also regulate pathways required for low oxygen adaptation and fungal virulence.

Author Contributions—R. B. conducted the experiments except as noted below, analyzed the results, and wrote the paper. E. V. S. conducted preliminary experiments and provided results for the deletion collection screen and microarray experiment. W. S. assisted with qPCR experiments. S. Z. assisted with the deletion collection screen. H. K. H. B. and C. S. E. performed the lipidomics experiments and analysis. P. J. E. conceived the project and wrote the paper. All authors reviewed the results and approved the final version of this manuscript.

Acknowledgments—We thank J. Hwang for critical reading of the manuscript, C. Talbot for microarray data analysis, and W. Lai and L. C. Hung from the Department of Pathology at the University of Texas Southwestern Medical Center at Dallas for generating monoclonal antibody 5B4 to Sre1.

References

1. Summons, R. E., Bradley, A. S., Jahnke, L. L., and Waldbauer, J. R. (2006) Steroids, triterpenoids and molecular oxygen. *Philos. Trans. R. Soc. Lond. B Biol. Sci.* **361,** 951–968
2. Nakamura, M. T., and Nara, T. Y. (2004) Structure, function, and dietary regulation of Δ6, Δ5, and Δ9 desaturases. *Annu. Rev. Nutr.* **24,** 345–376
3. Kwast, K. E., Burke, P. V., and Poyton, R. O. (1998) Oxygen sensing and the transcriptional regulation of oxygen-responsive genes in yeast. *J. Exp. Biol.* **201,** 1177–1195
4. Horton, J. D., Goldstein, J. L., and Brown, M. S. (2002) SREBPs: transcriptional mediators of lipid homeostasis. *Cold Spring Harb. Symp. Quant. Biol.* **67,** 491–498
5. Nohturfft, A., DeBose-Boyd, R. A., Scheek, S., Goldstein, J. L., and Brown, M. S. (1999) Sterols regulate cycling of SREBP cleavage-activating protein (SCAP) between endoplasmic reticulum and Golgi. *Proc. Natl. Acad. Sci. U.S.A.* **96,** 11235–11240
6. Sakai, J., Nohturfft, A., Goldstein, J. L., and Brown, M. S. (1998) Cleavage of sterol regulatory element-binding proteins (SREBPs) at site-1 requires interaction with SREBP cleavage-activating protein–Evidence from *in vivo* competition studies. *J. Biol. Chem.* **273,** 5785–5793
7. Eberlé, D., Hegarty, B., Bossard, P., Ferré, P., and Foufelle, F. (2004) SREBP transcription factors: master regulators of lipid homeostasis. *Biochimie* **86,** 839–848
8. Hughes, A. L., Todd, B. L., and Espenshade, P. J. (2005) SREBP pathway responds to sterols and functions as an oxygen sensor in fission yeast. *Cell* **120,** 831–842
9. Todd, B. L., Stewart, E. V., Burg, J. S., Hughes, A. L., and Espenshade, P. J. (2006) Sterol regulatory element binding protein is a principal regulator of anaerobic gene expression in fission yeast. *Mol. Cell. Biol.* **26,** 2817–2831
10. Bien, C. M., and Espenshade, P. J. (2010) Sterol regulatory element binding proteins in fungi: hypoxic transcription factors linked to pathogenesis. *Eukaryot. Cell* **9,** 352–359
11. Bien, C. M., Chang, Y. C., Nes, W. D., Kwon-Chung, K. J., and Espenshade, P. J. (2009) *Cryptococcus neoformans* site-2 protease is required for virulence and survival in the presence of azole drugs. *Mol. Microbiol.* **74,** 672–690
12. Lee, H., Bien, C. M., Hughes, A. L., Espenshade, P. J., Kwon-Chung, K. J., and Chang, Y. C. (2007) Cobalt chloride, a hypoxia-mimicking agent, targets sterol synthesis in the pathogenic fungus *Cryptococcus neoformans. Mol. Microbiol.* **65,** 1018–1033
13. Blatzer, M., Barker, B. M., Willger, S. D., Beckmann, N., Blosser, S. J., Cornish, E. J., Mazurie, A., Grahl, N., Haas, H., and Cramer, R. A. (2011) SREBP coordinates iron and ergosterol homeostasis to mediate triazole drug and hypoxia responses in the human fungal pathogen *Aspergillus fumigatus*. *PLoS Genet.* **7,** e1002374
14. Willger, S. D., Cornish, E. J., Chung, D., Fleming, B. A., Lehmann, M. M., Puttikamonkul, S., and Cramer, R. A. (2012) Dsc orthologs are required for hypoxia adaptation, triazole drug responses, and fungal virulence in *Aspergillus fumigatus. Eukaryot. Cell* **11,** 1557–1567
15. Willger, S. D., Puttikamonkul, S., Kim, K. H., Burritt, J. B., Grahl, N., Metzler, L. J., Barbuch, R., Bard, M., Lawrence, C. B., and Cramer, R. A., Jr. (2008) A sterol-regulatory element binding protein is required for cell polarity, hypoxia adaptation, azole drug resistance, and virulence in *Aspergillus fumigatus. PLoS Pathog.* **4,** e1000200
16. Lane, S., Di Lena, P., Tormanen, K., Baldi, P., and Liu, H. (2015) Function and regulation of Cph2 in *Candida albicans. Eukaryot. Cell* **14,** 1114–1126
17. DuBois, J. C., Pasula, R., Dade, J. E., and Smulian, A. G. (2016) Yeast transcriptome and *in vivo* hypoxia detection reveals *Histoplasma capsulatum* response to low oxygen tension. *Med. Mycol.* **54,** 40–58
18. Zhang, S., Skalsky, Y., and Garfinkel, D. J. (1999) *MGA2* or *SPT23* is required for transcription of the Δ9 fatty acid desaturase gene, *OLE1*, and nuclear membrane integrity in *Saccharomyces cerevisiae*. *Genetics* **151,** 473–483
19. Kandasamy, P., Vemula, M., Oh, C. S., Chellappa, R., and Martin, C. E. (2004) Regulation of unsaturated fatty acid biosynthesis in *Saccharomyces*: the endoplasmic reticulum membrane protein, Mga2p, a transcription activator of the *OLE1* gene, regulates the stability of the *OLE1* mRNA through exosome-mediated mechanisms. *J. Biol. Chem.* **279,** 36586–36592
20. Moreno, S., Klar, A., and Nurse, P. (1991) Molecular genetic analysis of fission yeast *Schizosaccharomyces pombe*. *Methods Enzymol.* **194,** 795–823
21. Stewart, E. V., Nwosu, C. C., Tong, Z., Roguev, A., Cummins, T. D., Kim, D. U., Hayles, J., Park, H. O., Hoe, K. L., Powell, D. W., Krogan, N. J., and Espenshade, P. J. (2011) Yeast SREBP cleavage activation requires the Golgi Dsc E3 ligase complex. *Mol. Cell* **42,** 160–171
22. Edgar, R., Domrachev, M., and Lash, A. E. (2002) Gene Expression Omnibus: NCBI gene expression and hybridization array data repository. *Nucleic Acids Res.* **30,** 207–210
23. Ejsing, C. S., Sampaio, J. L., Surendranath, V., Duchoslav, E., Ekroos, K., Klemm, R. W., Simons, K., and Shevchenko, A. (2009) Global analysis of the yeast lipidome by quantitative shotgun mass spectrometry. *Proc. Natl. Acad. Sci. U.S.A.* **106,** 2136–2141
24. Husen, P., Tarasov, K., Katafiasz, M., Sokol, E., Vogt, J., Baumgart, J., Nitsch, R., Ekroos, K., and Ejsing, C. S. (2013) Analysis of lipid experiments (ALEX): a software framework for analysis of high-resolution shotgun lipidomics data. *PLoS ONE* **8,** e0079736
25. Casanovas, A., Sprenger, R. R., Tarasov, K., Ruckerbauer, D. E., Hannibal-

Bach, H. K., Zanghellini, J., Jensen, O. N., and Ejsing, C. S. (2015) Quantitative analysis of proteome and lipidome dynamics reveals functional regulation of global lipid metabolism. *Chem. Biol.* **22,** 412–425
26. Benjamini, Y., and Hochberg, Y. (1995) Controlling the false discovery rate: a practical and powerful approach to multiple testing. *J. Royal Stat. Soc. Series B* **57,** 289–300
27. Johnson, B., and Brown, C. M. (1972) A possible relationship between the fatty acid composition of yeasts and the 'petite' mutation. *Antonie Van Leeuwenhoek* **38,** 137–144
28. Hughes, B. T., and Espenshade, P. J. (2008) Oxygen-regulated degradation of fission yeast SREBP by Ofd1, a prolyl hydroxylase family member. *EMBO J.* **27,** 1491–1501
29. Jiang, Y., Vasconcelles, M. J., Wretzel, S., Light, A., Martin, C. E., and Goldberg, M. A. (2001) *MGA2* is involved in the low-oxygen response element-dependent hypoxic induction of genes in *Saccharomyces cerevisiae*. *Mol. Cell. Biol.* **21,** 6161–6169
30. Kelley, R., and Ideker, T. (2009) Genome-wide fitness and expression profiling implicate Mga2 in adaptation to hydrogen peroxide. *PLoS Genet.* **5,** e1000488
31. Ferreira, T., Régnacq, M., Alimardani, P., Moreau-Vauzelle, C., and Bergès, T. (2004) Lipid dynamics in yeast under haem-induced unsaturated fatty acid and/or sterol depletion. *Biochem. J.* **378,** 899–908
32. Bloomfield, D. K., and Bloch, K. (1960) The formation of Δ9-unsaturated fatty acids. *J. Biol. Chem.* **235,** 337–345
33. Klein, H. P., Eaton, N. R., and Murphy, J. C. (1954) Net synthesis of sterols in resting cells of *Saccharomyces cerevisiae*. *Biochim. Biophys. Acta* **13,** 591
34. Jahnke, L., and Klein, H. P. (1983) Oxygen requirements for formation and activity of the squalene epoxidase in *Saccharomyces cerevisiae*. *J. Bacteriol.* **155,** 488–492
35. Holic, R., Yazawa, H., Kumagai, H., and Uemura, H. (2012) Engineered high content of ricinoleic acid in fission yeast *Schizosaccharomyces pombe*. *Appl. Microbiol. Biotechnol.* **95,** 179–187
36. Tarsio, M., Zheng, H., Smardon, A. M., Martínez-Muñoz, G. A., and Kane, P. M. (2011) Consequences of loss of Vph1 protein-containing vacuolar ATPases (V-ATPases) for overall cellular pH homeostasis. *J. Biol. Chem.* **286,** 28089–28096
37. Martínez-Muñoz, G. A., and Kane, P. (2008) Vacuolar and plasma membrane proton pumps collaborate to achieve cytosolic pH homeostasis in yeast. *J. Biol. Chem.* **283,** 20309–20319
38. Solaini, G., Baracca, A., Lenaz, G., and Sgarbi, G. (2010) Hypoxia and mitochondrial oxidative metabolism. *Biochim. Biophys. Acta* **1797,** 1171–1177
39. Spåhr, H., Samuelsen, C. O., Baraznenok, V., Ernest, I., Huylebroeck, D., Remacle, J. E., Samuelsson, T., Kieselbach, T., Holmberg, S., and Gustafsson, C. M. (2001) Analysis of *Schizosaccharomyces pombe* mediator reveals a set of essential subunits conserved between yeast and metazoan cells. *Proc. Natl. Acad. Sci. U.S.A.* **98,** 11985–11990
40. Conaway, R. C., and Conaway, J. W. (2011) Origins and activity of the mediator complex. *Semin. Cell Dev. Biol.* **22,** 729–734
41. Yang, F., Vought, B. W., Satterlee, J. S., Walker, A. K., Jim Sun, Z. Y., Watts, J. L., DeBeaumont, R., Saito, R. M., Hyberts, S. G., Yang, S., Macol, C., Iyer, L., Tjian, R., van den Heuvel, S., Hart, A. C., *et al.* (2006) An ARC/Mediator subunit required for SREBP control of cholesterol and lipid homeostasis. *Nature* **442,** 700–704
42. Ho, J. J., Metcalf, J. L., Yan, M. S., Turgeon, P. J., Wang, J. J., Chalsev, M., Petruzziello-Pellegrini, T. N., Tsui, A. K., He, J. Z., Dhamko, H., Man, H. S., Robb, G. B., Teh, B. T., Ohh, M., and Marsden, P. A. (2012) Functional importance of Dicer protein in the adaptive cellular response to hypoxia. *J. Biol. Chem.* **287,** 29003–29020
43. van den Beucken, T., Koch, E., Chu, K., Rupaimoole, R., Prickaerts, P., Adriaens, M., Voncken, J. W., Harris, A. L., Buffa, F. M., Haider, S., Starmans, M. H., Yao, C. Q., Ivan, M., Ivan, C., Pecot, C. V., *et al.* (2014) Hypoxia promotes stem cell phenotypes and poor prognosis through epigenetic regulation of DICER. *Nat. Commun.* **5,** 5203
44. Rupaimoole, R., Wu, S. Y., Pradeep, S., Ivan, C., Pecot, C. V., Gharpure, K. M., Nagaraja, A. S., Armaiz-Pena, G. N., McGuire, M., Zand, B., Dalton, H. J., Filant, J., Miller, J. B., Lu, C., Sadaoui, N. C., *et al.* (2014) Hypoxia-mediated downregulation of miRNA biogenesis promotes tumour progression. *Nat. Commun.* **5,** 5202
45. Fasanaro, P., D'Alessandra, Y., Di Stefano, V., Melchionna, R., Romani, S., Pompilio, G., Capogrossi, M. C., and Martelli, F. (2008) MicroRNA-210 modulates endothelial cell response to hypoxia and inhibits the receptor tyrosine kinase ligand Ephrin-A3. *J. Biol. Chem.* **283,** 15878–15883
46. Fasanaro, P., Greco, S., Lorenzi, M., Pescatori, M., Brioschi, M., Kulshreshtha, R., Banfi, C., Stubbs, A., Calin, G. A., Ivan, M., Capogrossi, M. C., and Martelli, F. (2009) An integrated approach for experimental target identification of hypoxia-induced miR-210. *J. Biol. Chem.* **284,** 35134–35143
47. Dang, K., and Myers, K. A. (2015) The role of hypoxia-induced miR-210 in cancer progression. *Int. J. Mol. Sci.* **16,** 6353–6372
48. Yang, W., Urano, J., and Tamanoi, F. (2000) Protein farnesylation is critical for maintaining normal cell morphology and canavanine resistance in *Schizosaccharomyces pombe*. *J. Biol. Chem.* **275,** 429–438
49. Song, J. Y., Cha, J., Lee, J., and Roe, J. H. (2006) Glutathione reductase and a mitochondrial thioredoxin play overlapping roles in maintaining iron-sulfur enzymes in fission yeast. *Eukaryot. Cell* **5,** 1857–1865
50. Song, J. Y., Kim, K. D., and Roe, J. H. (2008) Thiol-independent action of mitochondrial thioredoxin to support the urea cycle of arginine biosynthesis in *Schizosaccharomyces pombe*. *Eukaryot. Cell* **7,** 2160–2167
51. Kühl, I., Dujeancourt, L., Gaisne, M., Herbert, C. J., and Bonnefoy, N. (2011) A genome wide study in fission yeast reveals nine PPR proteins that regulate mitochondrial gene expression. *Nucleic Acids Res.* **39,** 8029–8041
52. Ryuko, S., Ma, Y., Ma, N., Sakaue, M., and Kuno, T. (2012) Genome-wide screen reveals novel mechanisms for regulating cobalt uptake and detoxification in fission yeast. *Mol. Genet. Genomics* **287,** 651–662
53. Kim, J., Ha, H. J., Kim, S., Choi, A. R., Lee, S. J., Hoe, K. L., and Kim, D. U. (2015) Identification of Rbd2 as a candidate protease for sterol regulatory element binding protein (SREBP) cleavage in fission yeast. *Biochem. Biophys. Res. Commun.* **468,** 606–610
54. Horton, J. D., Shah, N. A., Warrington, J. A., Anderson, N. N., Park, S. W., Brown, M. S., and Goldstein, J. L. (2003) Combined analysis of oligonucleotide microarray data from transgenic and knockout mice identifies direct SREBP target genes. *Proc. Natl. Acad. Sci. U.S.A.* **100,** 12027–12032
55. Henry, S. A., Kohlwein, S. D., and Carman, G. M. (2012) Metabolism and regulation of glycerolipids in the yeast *Saccharomyces cerevisiae*. *Genetics* **190,** 317–349
56. Převorovský, M., Oravcov´ M., Tvarůžková, J., Zach, R., Folk, P., Puta, F., and Bähler, J. (2015) Fission yeast CSL transcription factors: mapping their target genes and biological roles. *PLoS ONE* **10,** e0137820
57. Pancaldi, V., Saraç, O. S., Rallis, C., McLean, J. R., Převorovský, M., Gould, K., Beyer, A., and Bähler, J. (2012) Predicting the fission yeast protein interaction network. *G3* **2,** 453–467
58. Jarriault, S., Brou, C., Logeat, F., Schroeter, E. H., Kopan, R., and Israel, A. (1995) Signalling downstream of activated mammalian notch. *Nature* **377,** 355–358
59. Beres, T. M., Masui, T., Swift, G. H., Shi, L., Henke, R. M., and MacDonald, R. J. (2006) PTF1 is an organ-specific and notch-independent basic helix-loop-helix complex containing the mammalian suppressor of hairless (RBP-J) or its paralogue, RBP-L. *MCB* **26,** 117–130
60. Sakai, J., Rawson, R. B., Espenshade, P. J., Cheng, D., Seegmiller, A. C., Goldstein, J. L., and Brown, M. S. (1998) Molecular identification of the sterol-regulated luminal protease that cleaves SREBPs and controls lipid composition of animal cells. *Mol. Cell* **2,** 505–514
61. Hoppe, T., Matuschewski, K., Rape, M., Schlenker, S., Ulrich, H. D., and Jentsch, S. (2000) Activation of a membrane-bound transcription factor by regulated ubiquitin/proteasome-dependent processing. *Cell* **102,** 577–586
62. Radhakrishnan, A., Sun, L. P., Kwon, H. J., Brown, M. S., and Goldstein, J. L. (2004) Direct binding of cholesterol to the purified membrane region of SCAP: mechanism for a sterol-sensing domain. *Mol. Cell* **15,** 259–268
63. Hua, X., Nohturfft, A., Goldstein, J. L., and Brown, M. S. (1996) Sterol resistance in CHO cells traced to point mutation in SREBP cleavage-activating protein. *Cell* **87,** 415–426

64. Hannah, V. C., Ou, J., Luong, A., Goldstein, J. L., and Brown, M. S. (2001) Unsaturated fatty acids down-regulate SREBP isoforms 1a and 1c by two mechanisms in HEK-293 cells. *J. Biol. Chem.* **276,** 4365–4372
65. Grahl, N., Shepardson, K. M., Chung, D., and Cramer, R. A. (2012) Hypoxia and fungal pathogenesis: to air or not to air? *Eukaryot. Cell* **11,** 560–570
66. Bork, P., Doerks, T., Springer, T. A., and Snel, B. (1999) Domains in plexins: links to integrins and transcription factors. *Trends Biochem. Sci.* **24,** 261–263
67. Bork, P. (1993) Hundreds of ankyrin-like repeats in functionally diverse proteins: mobile modules that cross phyla horizontally? *Proteins* **17,** 363–374

Mga2 Transcription Factor Regulates an Oxygen-responsive Lipid Homeostasis Pathway in Fission Yeast

Risa Burr, Emerson V. Stewart, Wei Shao, Shan Zhao, Hans Kristian Hannibal-Bach, Christer S. Ejsing and Peter J. Espenshade

J. Biol. Chem. 2016, 291:12171-12183.
doi: 10.1074/jbc.M116.723650 originally published online April 6, 2016